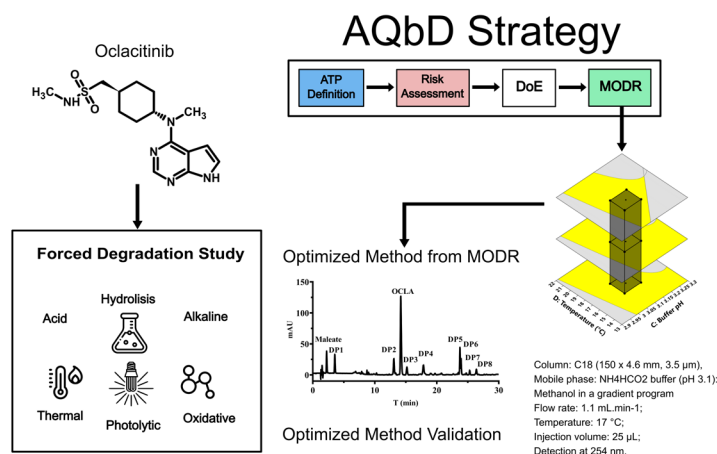


ARTICLE

# Development and Validation of a Stability-Indicating High-Performance Liquid Chromatography with Diode-Array Detection Method for Oclacitinib Using Analytical Quality by Design Approach

Dalton de Assis de Souza<sup>1</sup>, Danilo Raul Ossufo Momade<sup>1</sup>, Allan Michael Junkert<sup>1</sup>, Alexandre de Fátima Cobre<sup>1</sup>, Dile Pontarolo Stremel<sup>1</sup>, Raul Edison Luna Lazo<sup>1</sup>, Luana Mota Ferreira<sup>1</sup>, Roberto Pontarolo\*<sup>1</sup>

Programa de Pós-Graduação em Ciências Farmacêuticas, Universidade Federal do Paraná<sup>1</sup>, Av. Lothário Meissner, 632, 80210-170, Curitiba, PR, Brazil



This study aimed to develop and validate a stability-indicating method by high performance liquid chromatography to quantify the Oclacitinib (OCLA), on the presence of its degradation products (DPs), by applying Analytical Quality by Design (AQbD) strategy. OCLA was subjected to acidic, alkaline, neutral, photolytic, oxidative, and thermal stress conditions, with degradation products observed under acidic and photolytic conditions. After defining the Analytical Target Profile, the tailing factor, peak purity, and last peak retention time were established as Critical Quality Attributes. The risk assessment led to the designation of the mobile and stationary

phases, the oven temperature, the injection volume and the flow rate as Critical Method Parameters. A screening step was then performed to select categorical variables, and the significant factors were subsequently incorporated into the Box-Behnken Design for method optimization. The optimized method was achieved using Zorbax XBD C18 column (150 x 4.6 mm, 3.5  $\mu\text{m}$ ), oven temperature 17  $^{\circ}\text{C}$ , and injection volume 25  $\mu\text{L}$ . The mobile phase consisted of ammonium formate buffer 100 mM, pH 3.1 and methanol, and a flow rate of 1.1  $\text{mL min}^{-1}$ , eluted by a stepwise gradient. Furthermore, the method demonstrated excellent selectivity and linearity ( $R > 0.999$ ). The theoretical limit of detection was determined to be 5.52  $\mu\text{g mL}^{-1}$ , while the theoretical limit of quantification was found to be 16.74  $\mu\text{g mL}^{-1}$ . Furthermore, precision and accuracy were demonstrated with a relative standard deviation below 2.0% and accuracy ranging from 99.87% to 101.38%. Hence, the method was successfully developed, optimized, and validated by applying AQbD approach, becoming a useful methodology for routine quality control of OCLA and its degradation products.

**Cite:** de Souza, D. A.; Momade, D. R. O.; Junkert, A. M.; Cobre, A. F.; Stremel, D. P.; Lazo, R. E. L.; Ferreira, L. M.; Pontarolo, R. Development and Validation of a Stability-Indicating High-Performance Liquid Chromatography with Diode-Array Detection Method for Oclacitinib Using Analytical Quality by Design Approach. *Braz. J. Anal. Chem.* 2025, 12 (49), pp 67-89. <http://dx.doi.org/10.30744/brjac.2179-3425.AR-6-2024>

Submitted January 13, 2024; Resubmitted March 26, 2025; Accepted April 11, 2025; Available online May 21, 2025.

**Keywords:** Forced degradation, liquid chromatography, AQbD, Box-Behnken Design, Janus kinase inhibitor

## INTRODUCTION

Oclacitinib (OCLA), chemically known as N-methyl-1-[4-[methyl(7H-pyrrole[2,3-d]pyrimidine-4-yl)amino]cyclohexyl]methanesulfonamide (Figure 1), is a cyclohexylamine pyrrole derived from pyrimidine.<sup>1</sup> The OCLA functions by inhibiting the activity of Janus kinases 1 and 2 enzymes, which play a role in the signaling pathway involved in inflammatory and immune responses.<sup>2,3</sup> It was approved by the FDA in 2013 to prevent and treat pruritus related to allergic and atopic canine dermatitis.<sup>4,5</sup> Despite its significance, research on analytical methods to determine OCLA in active pharmaceutical ingredient (API) and different formulations is still scarce.

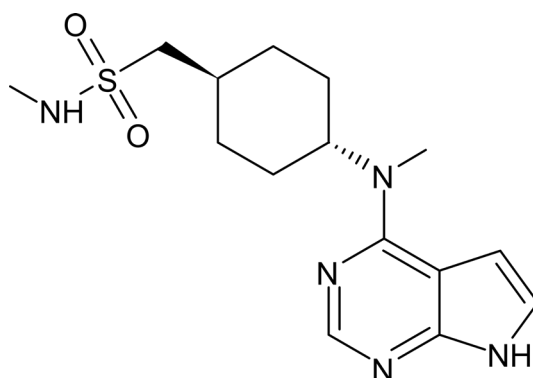


**Figure 1.** The chemical structure of Oclacitinib.

Stability studies aim to provide evidence on drug quality, assessing whether there is variation in the API content or changes in medication characteristics resulting from environmental factors including temperature, humidity, and storage conditions. These modifications are crucial as they directly impact both the drug's efficacy and safety. The presence of DPs may lead to sub-therapeutic doses and/or occurrence of adverse events.<sup>6</sup> Conducting stress tests on the drug compound aids in identifying potential DPs, thereby establishing decomposition pathways and inherent stability of the molecule. Furthermore, it validates the stability-indicating analytical method, ensuring the accurate quantification of the API amidst its degradation products and excipients without interference.<sup>7,8</sup>

A trial-based approach, also known as one-factor-at-a-time (OFaT), is still widely used to develop analytical methods by liquid chromatography. This approach involves altering a chromatographic parameter in each experiment until the desired outcome is achieved. However, it may increase the number of experiments required, as the process relies on the analyst's expertise to rationalize these adjustments. Alternatively, Analytical Quality by Design (AQbD) represents a systematic strategy for developing and validating analytical methods. This approach ensures quality, robustness, and efficiency through the application of risk assessment and multivariate analysis through the design of experiments (DOE).<sup>9-12</sup> Regulatory agencies have recognized the value of AQbD and supported its adoption. The United States Pharmacopeia (USP) is a modern directive that reflects the principles of AQbD, such as USP <1220> "The Analytical Procedure Lifecycle," which describes a sophisticated approach to analytical method development based on sound scientific procedures and quality risk management. Similarly, the International Council for Harmonization (ICH) has developed guidelines such as ICH Q14 and Q2(R2) that align with the AQbD framework, further emphasizing the industry's shift toward a more scientific and risk-based quality assurance model. In this context, the Analytical AQbD approach is directly compatible with ICH Q14 and USP GC <1220>, which advocate a lifecycle management framework for analytical procedures. This framework encompasses Procedure Design, Performance Qualification and Continuous Monitoring, ensuring method robustness and flexibility within predefined Method Operational Design Regions (MODRs).<sup>13,14</sup>

For instance, OCLA has been quantified in the plasma of dogs, cats, and horses through a pharmacokinetic study using liquid chromatography coupled to mass spectroscopy (LC-MS) technique.<sup>15–17</sup> Additionally, our group previously developed a spectrophotometric method for determining OCLA in capsule formulations.<sup>18</sup> To our knowledge, a stability-indicating method utilizing an AQbD approach for OCLA in API to monitor its stability has not been reported. This study aimed to develop a robust stability-indicating HPLC-DAD method based on AQbD for the quantification of OCLA in the presence of its degradation products. Following the establishment of Analytical Target Profiles (ATPs) and Critical Method Attributes (CMAs), a comprehensive risk assessment was conducted to identify and classify Critical Method Parameters (CMPs) as categorical or numerical variables. A screening study was performed to select categorical CMPs, including the type of buffer, organic solvent, and stationary phase, while a preliminary study established fundamental HPLC conditions, such as the initial organic phase ratio, initial organic phase hold time, detection wavelength, and injection volume. These studies also defined the experimental range for further modeling. The method optimization phase employed a Box–Behnken design, a response surface methodology, to evaluate the influence of CMPs on CMAs and establish a robust analytical region, with the optimized parameters positioned at its center. The final method was validated in accordance with ICH and ANVISA guidelines, ensuring its reliability and applicability for laboratory routine.

## **MATERIALS AND METHODS**

### ***Standard and reagents***

Oclacitinib standard was purchased (Nanjing Kaimubo, China, Batch No. 2023031601) with 99.06% purity. The ammonium acetate, HPLC grade acetonitrile (ACN), methanol (MeOH) and tetrahydrofuran (THF) were obtained from J.T.Baker® (New Jersey, USA), formic acid and ammonium formate were from Aldrich (Missouri, USA). Acetic acid and hydrogen peroxide (H<sub>2</sub>O<sub>2</sub>, 30%) was acquired from Labsynth (São Paulo, Brazil). Sodium hydroxide (NaOH) was acquired from ACS Científica (São Paulo, Brazil), and hydrochloric acid (HCl) was acquired from Neon Comercial (São Paulo, Brazil). Ultrapure water was obtained through the Milli-Q® Gradient A10-Millipore purification system (Milford, USA).

### ***Analytical instrumentation***

The analyses were conducted using an Agilent 1100 series HPLC system (Agilent Technologies, California, USA) coupled to a diode-array detector (DAD). The chromatograms were recorded and analyzed through an Agilent ChemStation® version B.04.03[16]. The method development process involved evaluating different combinations of stationary phase, mobile phase, organic modifier and mobile phase pH. The chromatographic columns tested included Agilent Zorbax Eclipse XDB C18 (4.6 mm × 150 mm, 3.5 µm), Waters XBridge BEH C8 (4.6 mm × 150 mm, 5 µm) and Waters Spherisorb® ODS2 (4.6 mm × 150 mm, 5 µm). The mobile phase was composed of 100 mM ammonium acetate buffer (pH 4.76) or ammonium formate buffer (pH 3.75) (mobile phase A), combined with organic solvents such as acetonitrile (ACN), methanol (MeOH) or tetrahydrofuran (THF) (mobile phase B). For monitoring OCLA in the stability tests, a Zorbax C18 (150 × 4.6 mm, 3.5 µm) column was utilized with ammonium formate buffer pH 3.2 and MeOH using a scouting gradient program (5%B at 0.0 min, 5%B from 0.0 to 5 min, 5-80%B from 5.0 to 55 min and 80-5%B from 55-57 min) delivered at 1 mL min<sup>-1</sup> flow rate. The analysis was conducted at 25 °C, with a 25 µL injection volume, and detection at 254 nm.

### ***Standard and sample preparation***

The stock solution of OCLA was prepared in MeOH to achieve a concentration of 1 mg mL<sup>-1</sup> and stored at -40 °C. For the stressing assays, the OCLA standard was prepared in MeOH with a stressing agent at a 50:50 (v/v) ratio, maintaining a final concentration of 1 mg mL<sup>-1</sup> and submitted to 60 °C. Prior to analysis, these solutions were neutralized if necessary, diluted with mobile phase to obtain a working solution with a concentration of 200 µg mL<sup>-1</sup>, and filtered through a 0.22 µm PTFE syringe filter before being subjected to chromatography.

### Forced degradation study

The degradation behavior of OCLA was acquired by subjecting the OCLA solution to various stress-inducing conditions, consisting of acid, alkaline, oxidative, photolytic, and thermal stress.<sup>13,19</sup> These assays were conducted under the following conditions: *i*) Hydrolytic stress (1 M HCl, 1 M NaOH, and neutral hydrolysis at 60 °C); *ii*) oxidative stress (3% H<sub>2</sub>O<sub>2</sub> at room temperature); *iii*) thermal stress (solid-state at 60 °C); and *iv*) photolytic stress (exposure to a light source option 2), in accordance with ICH recommendations.<sup>20</sup> The acid, alkaline, neutral hydrolysis, and oxidative stress tests were monitored for 7 days, thermal stress for 4 days, and photolytic stress for 1.75 days. The stability was assessed by monitoring the appearance of chromatographic peaks, the decrease in OCLA's peak area and comparison with control samples. Lastly, all DPs identified in the forced degradation assay were combined in equal proportions to produce the solution used for method development and optimization.

Preliminary tests were performed to previously establish some parameters such as detection wavelength and injection volume, in addition to a stable pH range to work with OCLA and its degradation products. The detection wavelength was established to allow the simultaneous observation of OCLA and the majority of its degradation products. An injection volume was determined to avoid interference of secondary and non-accumulative photolytic degradation products in the chromatogram, and a pH range was defined in which the ionization of OCLA degradation products remained stable.

### Development of the analytical method using the AQbD approach

The entire process, from ATP definition to validation, is summarized in Figure 2, which presents a flowchart of the AQbD strategy used for method development. All multivariate analyses were conducted using Design Expert v11.1 software.

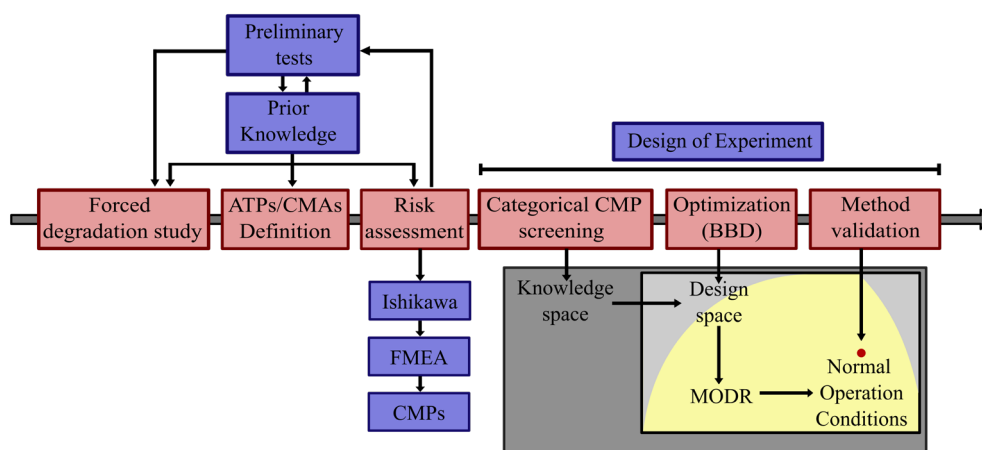


**Figure 2.** Flowchart of the AQbD method development process for OCLA.

### Establishment of analytical target profile and critical method attributes

An AQbD strategy was employed to develop a stability-indicating analytical method to estimate OCLA in the API among its DPs. The proposed Analytical Target Profile (ATP) was structured to outline the intended goals clearly. The ATP elements were categorized into characteristic and performance criteria, along with justifications and potential Critical Method Attributes (CMAs) associated with each element. These CMAs comprised OCLA's resolution, OCLA's adjacent peak resolution, OCLA's tailing factor, OCLA's capacity factor, and the last chromatographic peak capacity factor, intending to reduce the total run time. (Supplementary Figure S1).

### ***Risk assessment***

An Ishikawa diagram was proposed to identify parameters that may impact the method's quality. The risk assessment of these parameters was carried out using the Failure Modes and Effects Analysis (FMEA) methodology. In this process, each parameter was evaluated on a scale from 1 to 10, for three key criteria: occurrence, severity, and detection. The likelihood of variation in each parameter will be assessed to assign an occurrence score, while the severity score will determine the potential impact of any variation on the analytical results. The difficulty in detecting such variations will also be evaluated, leading to a detection score. These scores will be multiplied to calculate the Risk Priority Number (RPN) for each parameter.<sup>21,22</sup> Parameters with an RPN above 124 that cannot be addressed through preventive measures or resolved during preliminary tests will be classified as Critical Method Parameters (CMPs). The CMPs will then, be grouped into categorical and continuous variables, based on their nature.

### ***Categorical variables screening***

The categorical variables, including organic modifiers (ACN, MeOH and THF), mobile phase buffer (100 mM ammonium acetate buffer and 100 mM ammonium formate buffer), and stationary phases (Spherisorb® ODS2, XBridge BEH C8 and Zorbax Eclipse XBD C18), were combined and tested. The selection criteria for the combination were based on the OCLA capacity factor, with combinations exhibiting capacity factors outside the range of 3 to 15 being excluded. Additional factors considered included baseline stability, prioritizing combinations where the baseline remained stable without significant drift, and the absence of multiple coelutions, with combinations showing many overlapping peaks being discarded. Some OFaT experiments were conducted to establish the Initial Organic Ratio and Initial Organic Hold Time, which were optimized to minimize the loss of the acid degradation product in the dead volume.

### ***Optimization***

All the experiments were modeled using Analysis of Variance (ANOVA). The goodness of fit was evaluated based on model significance (p-value < 0.05), lack-of-fit (p-value > 0.05), and higher determination coefficients ( $R^2$ ,  $R^2$ -adj, and  $R^2$ -pred). After establishing the regression for each CMA, the corresponding polynomial equations were used in an overlay plot with quality thresholds, including OCLA's resolution and OCLA's adjacent peak resolution greater than 3, OCLA's tailing factor between 0.8 and 1.5, and last chromatographic peak capacity factor below 22.1. The region encompassing the threshold compliances was designated as the method operable design range (MODR). The normal operating conditions (NOC) and the proven acceptable ranges (PAR's) were selected within this region and tested to evaluate the regression's ability to predict the experiments. The NOC and PARs were validated by comparing the CMA results with the tolerance interval (TI), using a 95% confidence level and a 99% tolerance proportion.

### ***Control strategy***

A control strategy was established to ensure the reliability of the optimized method by the definition of the system suitability of the analytical procedure. The system suitability acceptance criteria will be established by analyzing the variation of parameters at the PARs points.<sup>22-24</sup>

### ***Method validation***

The validation was conducted in accordance with the ICH Q2(R2) guideline (2005), and the RDC N° 166, from August 24, 2017, by ANVISA, encompassing selectivity, linearity, precision, accuracy, the limit of detection, and the limit of quantification.<sup>13,25</sup> Selectivity was evaluated by assessing spectral purity using the Chemstation peak purity function, the threshold was set at 99% of spectral peak purity. Linearity was assessed by analyzing three independent analytical curves at five levels of standard solution concentration, ranging from 80 to 240  $\mu\text{g mL}^{-1}$ . The regression model was evaluated using correlation ( $R$ ) and determination ( $R^2$ ) coefficients, residual normality by the Ryan-Joiner test and residual homoscedasticity by Levene's test. The significance of the coefficients (angular and linear) was tested using the Student's  $t$ -test, and the model



fit was evaluated through ANOVA. All statistical analyses were performed using Minitab® 17.1.0 (LEAD Technologies, North Carolina, USA) and Prism® 8 (GraphPad, Inc, California, USA). The limit of detection (LoD) and quantification (LoQ) were estimated from the calibration curve parameters, however, for operational purposes, the LoQ should be considered as the lowest concentration point on the calibration curve.

The method's accuracy and precision were assessed using the sample preparation protocol at three concentration levels (80, 160, and 240  $\mu\text{g mL}^{-1}$ ). Accuracy was determined by evaluating the percentage agreement between the values accepted as true values and the values obtained at the low, medium and high levels of the calibration curve. Repeatability of the analytical procedure was evaluated by calculating the relative standard deviation (RSD) at low, medium, and high concentration levels of the calibration curve under the same operating conditions over a short interval of time. Then, the intermediate precision was assessed by calculating the RSD of samples analyzed by different analysts on different days. The method was considered accurate if the recovery ranged between 98% and 102%, and precise if the data exhibited an RSD of less than 2% with similar variance for intermediate precision.<sup>13,25,26</sup>

## RESULTS AND DISCUSSION

### Forced degradation study

The degradation profile of OCLA was determined by subjecting the OCLA solution to acid, alkaline, hydrolytic, oxidative, photolytic and thermal degradation, resulting in the emergence of DPs under both acidic hydrolysis and photolytic conditions (Figure 3). The acidic condition generated a new DP (Figure 3A) with a retention time of 4.1 minutes, and the peak area of OCLA decreased by 19.13% during 7 days of exposure. Conversely, under photolytic stress (Figure 3B), seven DPs were observed across the chromatogram, indicating high sensitivity to light. The peak area of OCLA decreased by 41.08% during 42 h of photolytic exposure. Under alkaline, neutral, thermal, and oxidative stress conditions, no new chromatographic peaks emerged, and there was no notable decrease in the peak area of OCLA (less than 2%).

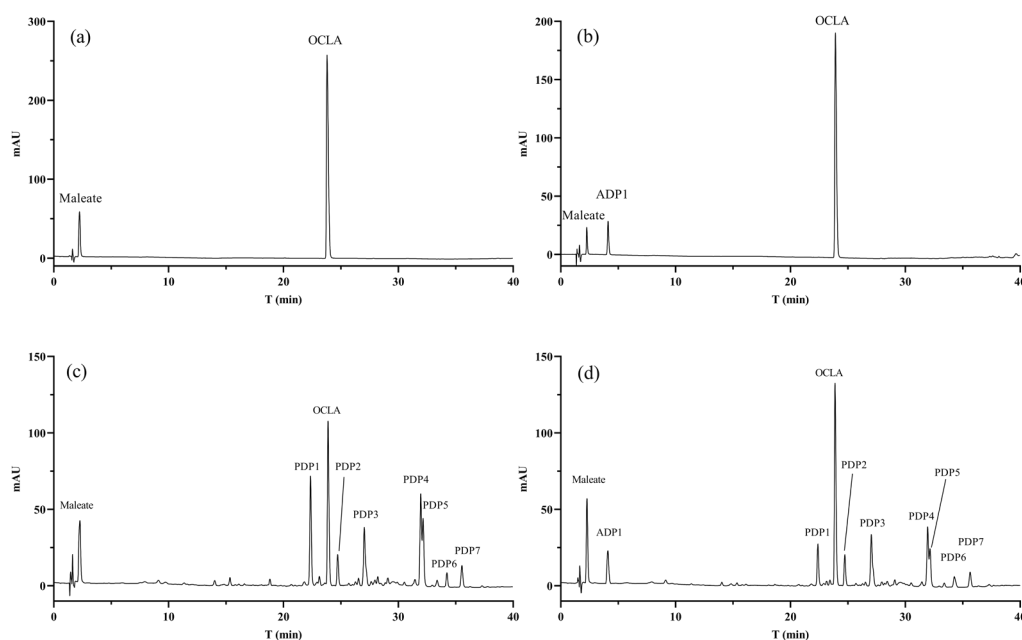


**Figure 3.** Chromatogram obtained from the stress conditions tested.

(Oclacitinib – OCLA; Acid Degradation Product – ADP; Photolytic Degradation Product – PDP) A - OCLA 200 mg B - HCl 1 M 60 °C, 7 days; C - Photolytic chamber (ICH's option 2), 44 hours; D - All degradation products combined. The chromatographic analysis was performed using a Zorbax XBD C18 column (150 × 4.6 mm, 3.5  $\mu\text{m}$ ). The mobile phase consisted of ammonium formate buffer pH 3.2 in combination with MeOH. A scouting gradient program was employed, with the following elution profile: 5%B at 0.0 min, 5%B from 0.0 to 5 min, 5-80%B from 5.0 to 55 min and 80-5%B from 55-57 min. The flow rate was maintained at 1.0 mL min<sup>-1</sup> throughout the analysis. The analysis was conducted at 25 °C, with a 25  $\mu\text{L}$  injection volume, and detection at 254 nm.

### **Development of the analytical method employing the AQbD strategies**

The development of the analytical target represents the initial steps in establishing the objectives and the required performance criteria for the method (Table I).<sup>27</sup> Based on these criteria, the CMAs were established, which directly correlate with the main goal of the method - To develop and validate an RP-HPLC-DAD method with stability-indicating properties for the detection and quantification OCLA avoiding interference from DPs (CMAs - OCLA's resolution and OCLA's adjacent peak resolution) ensuring the absence of chromatographic issues (CMA - OCLA's tailing factor), and minimizing analysis time (CMA - last chromatographic peak capacity factor).

**Table I.** Analytical target profile elements for the development of the stability-indicating method

| <b>Purpose of the method</b>   |  |   |  |
|--|--|---|--|
| To develop and validate a stability-indicating RP-HPLC-DAD method capable of detecting and quantitating Oclacitinib without chromatographic issues, avoiding interference from degradation products, and minimizing analysis time. |  |   |  |
| <b>ATP element</b>   | <b>Target</b>                                    | <b>Justification</b>  | <b>Related CMA</b>                                   |
| <b>Characteristic Criteria</b>   |  |   |  |
| Sample   | OCLA API   | Development of the indicative stability method for OCLA in the form of the active pharmaceutical ingredient.  | –  |
| Separation   | Reversed-phase LC                                | Oclacitinib is a low polarity drug, and as a result, the reverse phase is often employed for its analysis.  | –  |
| Detection  | UV-vis   | The oclacitinib structure has a chromophore so that the diode array detector may be applied.  | –  |
| Method application   | Stability study                                  | The method applied to quantify oclacitinib among its degradation products in stability tests.   | –  |
| <b>Performance Criteria – Categorical Variables</b>  |  |   |  |
| Retention time optimization  | OCLA's Optimal Retention                         | Ensuring OCLA's retention time falls within the optimal range is critical for consistent separation, minimizing overlapping peaks, and improving detection reliability.     | OCLA's capacity factor > 3 and < 15                  |
| Chromatographic issue  | Stable Baseline                                  | A stable baseline is required to avoid interference with detection and quantification   | Baseline Issues (+ or -)                             |
| Absence of interference  | Little or no coelution                           | Multiple co-elutions in the early stages of method development can lead to difficulty in obtaining proper resolution  | Multiple Co-elutions (+ or -)                        |
| <b>Performance Criteria – Continuous Variables</b>   |  |   |  |
| Resolution of Critical Pairs   | Clear Separation between OCLA and adjacent peaks | Clear separation between oclacitinib and critical peaks prevents co-elution, ensuring accurate and reliable quantification by avoiding interference from adjacent compounds | OCLA's resolution and adjacent peak resolution (> 3) |

(continues on next page)

**Table I.** Analytical target profile elements for the development of the stability-indicating method (continuation)

| ATP element                                 | Target                        | Justification  | Related CMA  |
|---|-------------------------------|--|--|
| Performance Criteria – Continuous Variables |                               |  |  |
| Peak Symmetry                               | Reduce OCLA's tailing         | Tailing in chromatographic peaks may affect the method's accuracy and precision, leading to quantification issues. | OCLA's tailing factor (0.8-1.5)                        |
| Time of analysis                            | Reduce total time of analysis | Reducing the total analysis time can result in mobile phase savings.   | Capacity factor of the last chromatographic peak (<3Q) |

ATP = Analytical target profile, OCLA = Oclacitinib, API = active pharmaceutical ingredient.

The Ishikawa diagram was used to identify parameters that may impact the quality of the method (Supplementary Figure S1). The potential critical method parameters found were grouped into method, sample preparation, mobile phase characteristics, detection and analysis, equipment and environment. These parameters had their degree of risk assessed through the application of the FMEA tool, where Risk Priority Number thresholds were considered as follows: >225 (high risk), 224–175 (unacceptable), 174–125 (need evaluation), 124–50 (acceptable), and <50 (negligible) (see supplementary table SI). This analysis identified the stationary phase, organic modifier, mobile phase buffer, oven temperature, flow rate, mobile phase pH, mobile phase gradient slope, injection volume, and wavelength as critical factors to the method. Other studies have also demonstrated that these variables are commonly considered critical parameters in method development.<sup>28–30</sup>

A screening step was conducted to select the categorical variables, which included the chromatographic column, organic modifier, and mobile phase buffer. The combination of Eclipse XDB C18, MeOH, and ammonium formate 100 mM (pH 3.0) (Supplementary figure S2A) yielded the most favorable profile regarding OCLA's capacity factor, peak resolutions and chromatogram baseline.

To reduce the dimensional space design, some of the continuous variables, such as the injection volume, wavelength, initial organic ratio and hold time were previously tested and fixed at 25  $\mu$ L, 254 nm, 5% and 4 min respectively. Initial tests showed that the analytes were divided into three sections along the chromatogram, an initial analyte for which the initial organic ratio and hold time were optimized, and two groups with four analytes each. To facilitate the modeling of resolution in critical pairs and reduce execution time, a stepwise gradient was developed, in which each of the previously mentioned groups of four analytes was assigned to a specific gradient segment with a defined slope. The slope corresponding to the segment containing only degradation products was fixed at 1.0 [% organic]  $\text{min}^{-1}$ , while the slope of the segment where OCLA elutes was taken to be modeled and optimized. A challenge identified during preliminary tests was the abrupt variation in the capacity factor of a degradation product adjacent to OCLA, depending on the pH applied. This change, likely resulting from an alteration in the molecule's ionization state, was observed around pH 3.3. Considering this effect and the fact that pH values above 3.3 led to the coelution of OCLA with this specific degradation product, the pH range selected for modeling was restricted to values below this threshold.

Finally, the ranges for the continuous variables were defined as follows: gradient slope (0.8–1.2 [% organic]  $\text{min}^{-1}$ ), flow rate (1.0–1.2  $\text{mL min}^{-1}$ ), buffer pH (3.0–3.2), and oven temperature (15–20  $^{\circ}\text{C}$ ). These ranges were applied on the Box-Behnken Design (BBD) to model the method and further optimize it. The stepwise approach ensured that the final method achieved the desired resolution and minimized analysis time. The BBD consisted of 28 experiments described in Supplementary Table SII.

The regression models along with their corresponding statistical parameters for each evaluated CMA are detailed in Table II. The data modeling indicated that a linear model best explained for the last peak capacity factor, the 2FI model more accurately described OCLA's tailing factor, and quadratic models were more suitable for OCLA's resolution and the resolution of its adjacent peak. Factors included in the model were selected based on the adjusted R-squared criterion, applying an output alpha of 0.05. During model



development, transformations such as square root, natural log, base 10 log, inverse, and inverse square root were tested, but none provided a significantly better fit than the raw data. For all modeled CMAs, the statistical analysis confirmed that the models were significant ( $p$ -value  $< 0.05$ ) and showed no lack of fit ( $p$ -value  $> 0.05$ ), suggesting that the model fits the data well and the variability is likely due to random errors. The  $R^2$  values of 0.9912, 0.9810, 0.8762, and 0.9639 for OCLA's resolution, OCLA's adjacent peak resolution (APR), OCLA's tailing factor, and last peak capacity factor, respectively, indicate that the model effectively captures the variability in the data. Furthermore, the  $R^2$ -adj values of 0.9881, 0.9767, 0.8473, and 0.9691 support the inclusion of the coefficients in the model, as their similarity to the  $R^2$  values of 0.9912, 0.9810, 0.8812 and 0.9736 indicates a low likelihood of overfitting. This assessment is further reinforced by the  $R^2$ -pred values of 0.9681, 0.9691, 0.8408, and 0.9600, which indicate strong predictive performance and consistency in the model's generalization capability.

**Table II.** Regression model of Box-Behnken Design experiments. A: mobile phase gradient slope; B: flow rate; C: buffer pH; D: oven temperature; Coef: term coefficients APR – adjacent peak resolution

| OCLA's Resolution         |        |           | OCLA's APR                |        |           | OCLA's Tailing            |        |           | Last Peak Capacity factor |        |           |
|---------------------------|--------|-----------|---------------------------|--------|-----------|---------------------------|--------|-----------|---------------------------|--------|-----------|
| Quadratic model           |        |           | Quadratic model           |        |           | 2FI Model                 |        |           | Linear Model              |        |           |
| Param                     | Coef   | p-value   | Param                     | Coef   | p-value   | Param                     | Coef   | p-value   | Param                     | Coef   | p-value   |
| A                         | -0.363 | $< 0.001$ | A                         | -0.073 | $< 0.001$ | A                         | -0.020 | $< 0.001$ | A                         | -2.090 | $< 0.001$ |
| B                         | 0.151  | $< 0.001$ | B                         | -0.116 | $< 0.001$ | C                         | -0.044 | $< 0.001$ | B                         | 2.170  | $< 0.001$ |
| C                         | -0.971 | $< 0.001$ | C                         | 0.211  | $< 0.001$ | D                         | 0.009  | 0.048     | C                         | 0.087  | 0.010     |
| D                         | -0.339 | $< 0.001$ | D                         | 0.080  | $< 0.001$ | AC                        | -0.022 | 0.008     | -                         | -      | -         |
| BC                        | -0.107 | 0.018     | C <sup>2</sup>            | -0.055 | $< 0.001$ | AD                        | -0.018 | 0.021     | -                         | -      | -         |
| A <sup>2</sup>            | 0.100  | 0.005     | -                         | -      | -         | CD                        | 0.017  | 0.028     | -                         | -      | -         |
| C <sup>2</sup>            | 0.307  | $< 0.001$ | -                         | -      | -         | -                         | -      | -         | -                         | -      | -         |
| Model                     |        | $< 0.001$ | Model                     |        | $< 0.001$ | Model                     |        | $< 0.001$ | Model                     |        | $< 0.001$ |
| Lack of fit               |        | 0.0726    | Lack of fit               |        | 0.6893    | Lack of fit               |        | 0.9696    | Lack of fit               |        | 0.2779    |
| R <sup>2</sup>            |        | 0.9912    | R <sup>2</sup>            |        | 0.9810    | R <sup>2</sup>            |        | 0.8812    | R <sup>2</sup>            |        | 0.9639    |
| R <sup>2</sup> -adjusted  |        | 0.9881    | R <sup>2</sup> -adjusted  |        | 0.9767    | R <sup>2</sup> -adjusted  |        | 0.8473    | R <sup>2</sup> -adjusted  |        | 0.9594    |
| R <sup>2</sup> -predicted |        | 0.9681    | R <sup>2</sup> -predicted |        | 0.9691    | R <sup>2</sup> -predicted |        | 0.8408    | R <sup>2</sup> -predicted |        | 0.9491    |

By analyzing the regression coefficients, related to the parameters and the parameter-interactions of the models of each CMA, it is possible to evaluate the effects of the CMPs and their interaction on the CMAs.<sup>31–33</sup> The buffer pH had a significant impact on the resolution of OCLA and its critical pairs, displaying an inverse relationship with OCLA Resolution but a direct proportional relationship with OCLA APR. This highlights the importance of carefully adjusting this CMP to achieve a balanced resolution. Additionally, the gradient slope influenced the Last Peak Retention Factor, while the flow rate affected both this response and the OCLA APR.

The MODR represents the range within which the combination of variables ensures the suitability of the analytical procedure for its intended application, as defined by the established CMAs. The MODR graph delineates a boundary that separates the regression model from the CMAs, signaling that the results fall within the acceptable range.<sup>34</sup> This robust region ensures the quality of the method by allowing adjustments within these defined limits. The quality verification of the method can be performed through a univariate test on experimental points to assess their concordance with the regression model.<sup>34,35</sup>

Once the model was fitted, the regressions were combined into an overlay plot (Figure 4). This plot was used to establish the quality thresholds for the CMAs, which included OCLA's Resolution and OCLA's APR below 3, OCLA's tailing factor between 0.8 and 1.5 and last peak capacity factor below 22.1. The MODR is depicted as the yellow area, where all CMAs meet the specified criteria.

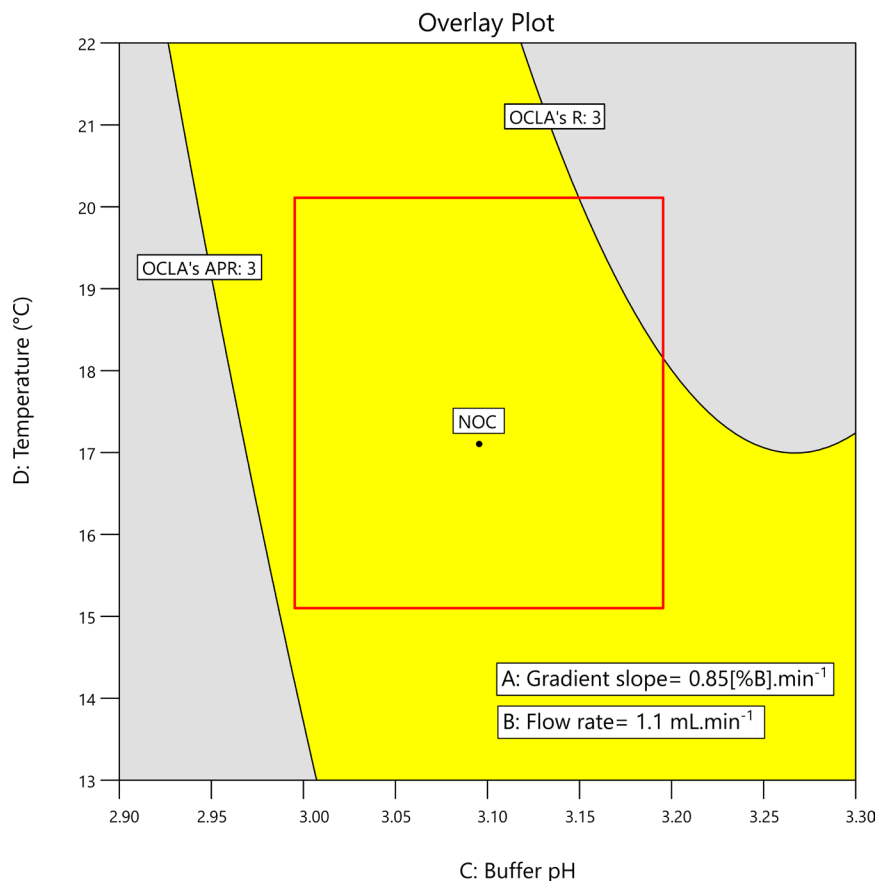


**Figure 4.** Overlay plot depicting the method operable design range and normal operating conditions. The area in the red square represents the Box-Behnken experimental range, while the black dot indicates the normal operating conditions.

Within the MODR, the PARs were established alongside the Normal Operating Conditions (NOC) to validate the model. The NOC was defined as comprising a mobile phase gradient slope of 0.85 [% organic] min<sup>-1</sup>, a flow rate of 1.1 mL min<sup>-1</sup>, a buffer pH of 3.1, and an oven temperature of 17 °C. The PARs (Supplementary figure S3) were defined as a fixed gradient slope of 0.85 [% organic] min<sup>-1</sup>, a flow rate range of 1.0 to 1.2 mL min<sup>-1</sup>, a buffer pH range of 3.05 to 3.15, and an oven temperature range of 16 to 18 °C. The tested points within the PARs, including the NOC, along with their corresponding results, are detailed in Supplementary Table SIII. The results obtained for the NOC and PARs demonstrate the robustness and validity of the model in predicting experimental results. The NOC and all PARs yielded results within the TI (95% confidence interval and 99% tolerance proportion) for all CMAs, except for the tailing factor, where PARs 2, 3, and 13 exceeded the predicted TI. Although most PARs produced results consistent with the model predictions for tailing factor, the occurrence of values outside the TI, together with the proximity of the results to the upper limit of the TI, suggests a slight tendency of the model to underestimate this CMA, indicating the presence of interactions not fully captured by the model. However, this does not compromise the applicability of the model, as most of the experimental results remain within the TI limits and all results remain within the acceptability criteria for tail factor (0.8 - 1.5).

The high reproducibility of the NOC metrics highlights the stability and reliability of the method at its optimal operating point. Overall, the model's predictive performance within the PARs and NOC supports its utility for method control and validation, while minor regions of variability suggest opportunities for further refinement to increase accuracy across the operating space.

A control strategy was established to ensure the method's reliability by defining system suitability criteria based on variations observed within the PARs. System suitability thresholds were determined from development and validation data, ensuring robustness in routine analysis.<sup>22–24</sup> The OCLA tailing factor varied between 1.262 and 1.405, the capacity factor ranged from 9.38 to 11.14, and the theoretical plates exceeded 34163, leading to the following acceptance criteria: tailing factor <1.405, capacity factor 9.38–11.14, and theoretical plates >34163. These system suitability criteria can be associated with control charts for continuous monitoring of the method. In this way, recurring deviations from the system suitability criteria can indicate problems such as equipment wear or column degradation, allowing timely maintenance or adjustments to ensure consistent method performance.

Figure 5 shows the NOC chromatogram that demonstrated the compliance of all CMAs in MODR. The final optimized method was achieved using an Zorbax C18 (150 x 4.6 mm, 3.5  $\mu$ m), mobile phase consisting of ammonium formate buffer 100 mM pH 3.1 with MeOH in a gradient program (5%B at 0.00 min, 5%B from 0.00 to 4.00 min, 5–25%B from 4.00 to 6.00 min, 25–37%B from 6.00 to 20.12 min, 37–45%B from 20.12 to 21.12 min, 45–55%B from 21.12 to 33.12 min, and 55–5%B from 33.12 to 37.12 min), with a flow rate of 1.1 mL min<sup>-1</sup>, injection volume of 25  $\mu$ L, the temperature set at 17 °C, and detection carried out at a wavelength of 254 nm. The DP1 shown in Figure 5 represents the OCLA's acidic stress degradation product, while the other seven originate from photolytic stress degradation products.

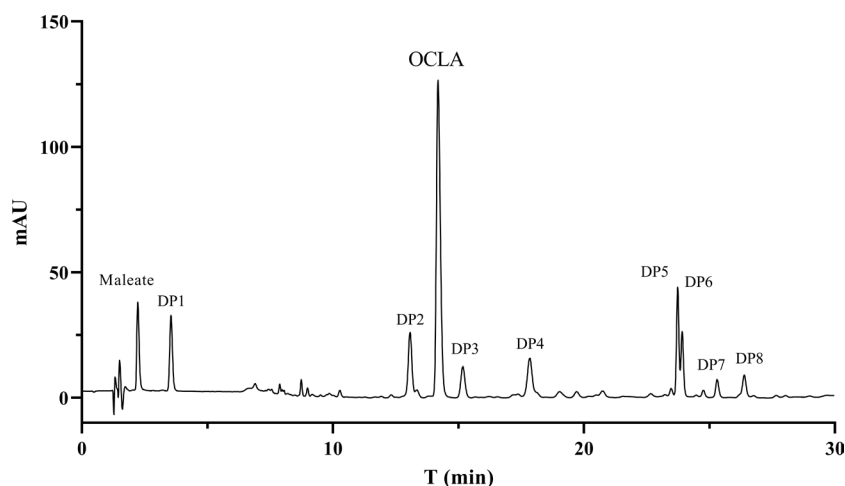


**Figure 5.** Stability-indicating method of Oclacitinib.

Chromatographic conditions: Zorbax C18 (150 x 4.6 mm, 3.5  $\mu$ m), mobile phase consisting of ammonium formate buffer 100mM pH 3.1 with MeOH in a gradient program (5%B at 0.00 min, 5%B from 0.00 to 4.00 min, 5–25%B from 4.00 to 6.00 min, 25–37%B from 6.00 to 20.12 min, 37–45%B from 20.12 to 21.12 min, 45–55%B from 21.12 to 33.12 min, and 55–5%B from 33.12 to 37.12 min) with a flow rate of 1.1 mL.min<sup>-1</sup>. The analysis was conducted at 17 °C, with a 25  $\mu$ L injection volume, and detection at 254 nm. DP1 from acidic stress; DP2–8 from photolytic stress.

### Method validation

The method demonstrated selectivity by ensuring there was no chromatographic peak overlap in the analysis of the OCLA sample. Each substance exhibited a distinct retention time. Additionally, the use of the peak purity tool revealed that the spectral congruence of the OCLA exceeded 99% in the NOC.

The regression analysis demonstrated linearity within the 80 to 240  $\mu$ g mL<sup>-1</sup> concentration range, displaying a strong correlation ( $R = 0.999$ ;  $R^2 = 0.999$ ). Linearity calibration curves can be viewed in Supplementary Figure S4. The Ryan-Joiner and Levene's tests yielded p-values >0.05, confirming the normal distribution and homogeneity of residuals. A regression fit with p-value below 0.05 indicates the statistical significance of the linear model concerning OCLA's content. The lack-of-fit parameter's p-value was above 0.05, suggesting

randomness in errors. The angular coefficient demonstrated deviation from zero ( $p$ -value  $< 0.05$ ), while the intercept showed no significant deviation from zero ( $p$ -value  $> 0.05$ ). Table III presents the parameters of the regression analysis.

**Table III.** Regression analysis of Oclacitinib. CI = Confidence interval, Sy.x = Standard error of estimate, LoD = Limit of detection, LoQ = Limit of Quantification.

| Parameter           | Value                             | p-value   |
|---------------------|-----------------------------------|-----------|
| Equation            | $Y = 13.564 \cdot X - 47$         |           |
| Range               | 80 - 240 $\mu\text{g mL}^{-1}$    |           |
| R                   | 0.999                             |           |
| R <sup>2</sup>      | 0.999                             |           |
| Angular coefficient | 13.564<br>(CI 95% = 13.02-14.11)  | $< 0.001$ |
| Linear coefficient  | -47<br>(CI 95% = -139,0 to 45,00) | 0.041     |
| Sy.x                | 21,55                             |           |
| LoD                 | 5.24 $\mu\text{g mL}^{-1}$        |           |
| LoQ                 | 15.89 $\mu\text{g mL}^{-1}$       |           |
| Model fit           |                                   | $< 0.001$ |
| Lack-of-fit         |                                   | 0.1       |

The limits of detection (LoD) and quantification (LoQ) were established based on the calibration curve parameters, using the standard error of estimate. The LoD was determined to be 5.24  $\mu\text{g mL}^{-1}$ , while the LoQ was calculated as 15.89  $\mu\text{g mL}^{-1}$ .

Precision was evaluated through both repeatability and intermediate precision analyses. Repeatability findings are presented in Supplementary Table SIV, with a calculated RSD of less than 2%, indicating low variability. Additionally, intermediate precision (Supplementary Table SV) was evaluated using Student's  $t$ -test and F-test to compare means and variances between different days. The comparison showed no statistical significance, with  $p$ -values greater than 0.05. The accuracy of the method was evaluated based on data agreement, employing three concentration levels outlined in Table SVI. The results demonstrated recoveries of  $98.05\% \pm 0.14\%$ ,  $99.85\% \pm 0.32\%$ , and  $99.07\% \pm 0.50\%$  for the low, medium, and high concentration levels, respectively ( $n = 3$ , 95% CI), with RSD values below 2%, confirming the method's accuracy.<sup>13,26</sup>

## Discussion

As previously mentioned, current pharmacokinetic studies in dogs, cats and horses have frequently employed LC-MS methods for the quantification of Oclacitinib in plasma.<sup>15–17</sup> Although LC-MS methods have high sensitivity, their application in laboratory routines may be limited due to their high cost and the need for highly specialized equipment and operators. Alternative methods, such as UV spectrophotometry, have also been reported, but they present lower selectivity.<sup>18</sup>

In comparison, the method developed in this study provides a reliable, selective and low-cost alternative for the determination of OCLA and detection of its degradation products. In addition, the model with which this method was developed has a well-defined MODR, providing greater flexibility and analytical predictability, ensuring stability of the CMAs in the face of small changes in chromatographic parameters.

The robustness of the method was ensured by identifying and evaluating CMPs and their impact on CMAs. The use of a BBD to generate a response surface allowed the definition of a reliable operating space, where small variations in the mobile phase gradient, oven temperature, and flow do not compromise the resolution or the shape of the analytical peaks of OCLA. This stability allows operational adjustments to be made without the need for new regulatory validations, which is an important differential for the application of the method in the pharmaceutical industry.<sup>9–12</sup> Previous studies using AQbD have also demonstrated this advantage, allowing greater reproducibility and predictability of analytical methods.<sup>22,28–30,36</sup>

Despite the effectiveness of the method, some limitations can be explored in future studies. The present work focused on the determination of OCLA in API, but further investigations can evaluate the performance of the method in pharmaceutical formulations, such as tablets and oral suspensions. Another possible application is the quantification of OCLA in biological matrices (plasma, urine, tissues) for bioavailability and pharmacokinetic studies.

## CONCLUSION

Oclacitinib was found to be sensitive to photolytic and acidic stress, while oxidative, thermal, alkaline, and neutral stress did not lead to the generation of degradation products or decrease in API content. Eight DPs were detected, with seven arising from photolytic stress and one from acidic stress. The AQbD approach offers enhanced knowledge about method development and a deeper understanding of the interactions among analytical variables, thereby contributing to the overall method quality.

In addition, applying AQbD concepts not only leads to cost savings and faster method development but also allows for continuous improvement of the method through adjustments in MODR. The final optimized method utilized an Zorbax XBD C18 (150 x 4.6 mm, 3.5  $\mu$ m), mobile phase consisting of ammonium formate buffer 100 mM pH 3.1 with MeOH in a gradient program (5%B at 0.00 min, 5%B from 0.00 to 4.00 min, 5–25%B from 4.00 to 6.00 min, 25–37%B from 6.00 to 20.12 min, 37–45%B from 20.12 to 21.12 min, 45–55%B from 21.12 to 33.12 min, and 55–5%B from 33.12 to 37.12 min) a flow rate of 1.1 mL min<sup>-1</sup>, injection volume of 25  $\mu$ L, the temperature set at 17 °C, and detection wavelength of 254 nm.

This optimized method was undergoing successful validation and confirming its selectivity, linearity, precision, accuracy, and robustness. As a result, it can be effectively employed for the quantification of OCLA with its degradation products.

## Conflicts of interest

No conflicts of interest to disclose.

## Acknowledgements

The authors express their gratitude to the Brazilian National Council of Technological and Scientific Development (CNPq) and “Coordenação de Aperfeiçoamento de Pessoal de Nível Superior – Brasil” (CAPES) -Finance Code 001.

## REFERENCES

- (1) Roskoski, R. Janus Kinase (JAK) Inhibitors in the Treatment of Inflammatory and Neoplastic Diseases. *Pharmacol. Res.* **2016**, *111*, 784–803. <https://doi.org/10.1016/j.phrs.2016.07.038>
- (2) Santoro, D. Therapies in Canine Atopic Dermatitis. *Veterinary Clinics of North America: Small Animal Practice* **2019**, *49* (1), 9–26. <https://doi.org/10.1016/j.cvsm.2018.08.002>
- (3) Bäumer, W. Pharmacotherapy of Canine Atopic Dermatitis - Current State and New Trends. *Ankara Üniversitesi Veteriner Fakültesi Dergisi* **2019**, *67* (1), 107–111. <https://doi.org/10.33988/auvfd.644485>
- (4) Fukuyama, T.; Ganchingco, J. R.; Bäumer, W. Demonstration of Rebound Phenomenon Following Abrupt Withdrawal of the JAK1 Inhibitor Oclacitinib. *Eur. J. Pharmacol.* **2017**, *794*, 20–26. <https://doi.org/10.1016/j.ejphar.2016.11.020>



- (5) Haugh, I. M.; Watson, I. T.; Alan Menter, M. Successful Treatment of Atopic Dermatitis with the JAK1 Inhibitor Oclacitinib. *Baylor University Medical Center Proceedings* **2018**, 31 (4), 524–525. <https://doi.org/10.1080/08998280.2018.1480246>
- (6) Maggio, R. M.; Vignaduzzo, S. E.; Kaufman, T. S. Practical and Regulatory Considerations for Stability-Indicating Methods for the Assay of Bulk Drugs and Drug Formulations. *TrAC, Trends Anal. Chem.* **2013**, 49, 57–70. <https://doi.org/10.1016/j.trac.2013.05.008>
- (7) Zimmer, M. Forced Degradation and Long-Term Stability Testing for Oral Drug Products: A Practical Approach. In: Bajaj, S.; Singh, S. (Eds). *Methods for Stability Testing of Pharmaceuticals*. Part of the book series: Methods in Pharmacology and Toxicology (MIPT). Humana Press, New York, NY, 2018, pp 75–98. [https://doi.org/10.1007/978-1-4939-7686-7\\_4](https://doi.org/10.1007/978-1-4939-7686-7_4)
- (8) International Council for Harmonisation of Technical Requirements for Pharmaceuticals for Human Use. *Stability Testing of New Drug Substances and Products Q1A(R2)*, 2003. Available at: <https://database.ich.org/sites/default/files/Q1A%28R2%29%20Guideline.pdf> (accessed 2025-02-03).
- (9) Tome, T.; Žigart, N.; Časar, Z.; Obreza, A. Development and Optimization of Liquid Chromatography Analytical Methods by Using AQbD Principles: Overview and Recent Advances. *Org. Process Res. Dev.* **2019**, 23 (9), 1784–1802. <https://doi.org/10.1021/acs.oprd.9b00238>
- (10) Fukuda, I. M.; Pinto, C. F. F.; Moreira, C. dos S.; Saviano, A. M.; Lourenço, F. R. Design of Experiments (DoE) Applied to Pharmaceutical and Analytical Quality by Design (QbD). *Braz. J. Pharm. Sci.* **2018**, 54 (spe). <https://doi.org/10.1590/s2175-97902018000001006>
- (11) Veerubhotla, K.; Walker, R. B. Development and Validation of a Stability-Indicating RP-HPLC Method Using Quality by Design for Estimating Captopril. *Indian J. Pharm. Sci.* **2019**, 81 (1). <https://doi.org/10.4172/pharmaceutical-sciences.1000478>
- (12) Bhaskaran, N. A.; Kumar, L.; Reddy, M. S.; Pai, G. K. An Analytical “Quality by Design” Approach in RP-HPLC Method Development and Validation for Reliable and Rapid Estimation of Irinotecan in an Injectable Formulation. *Acta Pharm.* **2021**, 71 (1), 57–79. <https://doi.org/10.2478/acph-2021-0008>
- (13) International Council for Harmonisation of Technical Requirements for Pharmaceuticals for Human Use. *ICH Guideline Q2(R2) on Validation of Analytical Procedures*, 2022. Available at: [https://database.ich.org/sites/default/files/ICH\\_Q2-R2\\_Document\\_Step2\\_Guideline\\_2022\\_0324.pdf](https://database.ich.org/sites/default/files/ICH_Q2-R2_Document_Step2_Guideline_2022_0324.pdf) (accessed 2025-02-03).
- (14) United States Pharmacopeial Convention. *General Chapter <1220>: Analytical Procedure Life Cycle*. Rockville, 2022. [https://doi.org/10.31003/USPNF\\_M10975\\_02\\_01](https://doi.org/10.31003/USPNF_M10975_02_01)
- (15) Ferrer, L.; Carrasco, I.; Cristófol, C.; Puigdemont, A. A Pharmacokinetic Study of Oclacitinib Maleate in Six Cats. *Veterinary Dermatology* **2020**, 31 (2), 134–e24. <https://doi.org/10.1111/vde.12819>
- (16) Hunyadi, L.; Datta, P.; Rewers-Felkins, K.; Sundman, E.; Hale, T.; Fajt, V.; Wagner, S. Pharmacokinetics of a Single Dose of Oclacitinib Maleate as a Top Dress in Adult Horses. *J. Vet. Pharmacol. Ther.* **2022**, 45 (3), 320–324. <https://doi.org/10.1111/jvp.13043>
- (17) Collard, W. T.; Hummel, B. D.; Fielder, A. F.; King, V. L.; Boucher, J. F.; Mullins, M. A.; Malpas, P. B.; Stegemann, M. R. The Pharmacokinetics of Oclacitinib Maleate, a Janus Kinase Inhibitor, in the Dog. *J. Vet. Pharmacol. Ther.* **2014**, 37 (3), 279–285. <https://doi.org/10.1111/jvp.12087>
- (18) Momade, D. R. O.; Vilhena, R. de O.; Castro, C.; Regis, F.; Domingues, K. Z. A.; Schlichta, L. S.; Cobre, A. de F.; Pontarolo, R. Development and Validation of an UV-Vis Spectrophotometric Method for the Quantification of Oclacitinib in Capsule Formulation. *Revista de Ciências Farmacêutica Básica e Aplicadas - RCFBA* **2021**, 42. <https://doi.org/10.4322/2179-443X.0712>
- (19) Agência Nacional de Vigilância Sanitária (ANVISA). *RDC Nº 318 - Dispõe Sobre as Boas Práticas de Fabricação de Medicamentos*, 2019. Available at: [https://bvsms.saude.gov.br/bvs/saudelegis/anvisa/2019/rdc0318\\_06\\_11\\_2019.pdf](https://bvsms.saude.gov.br/bvs/saudelegis/anvisa/2019/rdc0318_06_11_2019.pdf) (accessed 2025-02-03).
- (20) Intl. Council for Harmonisation of Technical Requirements for Pharmaceuticals for Human Use. *ICH Topic Q1B Photostability Testing of New Active Substances and Medicinal Products Step 5*, 1996.
- (21) Mikulak, R. J.; McDermott, R.; Beauregard, M. *The Basics of FMEA* (2nd Ed.). Productivity Press, New York, 2017. <https://doi.org/10.1201/b16656>

- (22) Junkert, A. M.; Mieres, N. G.; Domingues, K. Z. A.; Ferreira, L. M.; Pontarolo, R. Development and Validation of a Stability-Indicating High-Performance Liquid Chromatography Method Coupled with a Diode Array Detector for Quantifying Haloperidol in Oral Solution Using the Analytical Quality-by-Design Approach. *J. Sep. Sci.* **2025**, *48* (1). <https://doi.org/10.1002/jssc.70067>
- (23) Lopes, I. J. N.; Fujimori, S. K.; Mendes, T. C.; de Almeida, R. A. D.; de Sousa, F. F. M.; de Oliveira, C. A.; do Nascimento, D. D.; Lourenço, F. R.; Rodrigues, M. I.; Prado, L. D. Application of Analytical Quality by Design (AQbD) for Stability-Indicating Method Development for Quantification of Nevirapine and Its Degradation Products. *Microchem. J.* **2024**, *199*. <https://doi.org/10.1016/j.microc.2024.109939>
- (24) Abdel-Moety, E. M.; Rezk, M. R.; Wadie, M.; Tantawy, M. A. A Combined Approach of Green Chemistry and Quality-by-Design for Sustainable and Robust Analysis of Two Newly Introduced Pharmaceutical Formulations Treating Benign Prostate Hyperplasia. *Microchem. J.* **2021**, *160*. <https://doi.org/10.1016/j.microc.2020.105711>
- (25) Agência Nacional de Vigilância Sanitária (ANVISA). *Resolução RDC Nº 166 – Dispõe Sobre a Validação de Métodos Analíticos e dá Outras Providências*, 2017. Available at: [https://bvsms.saude.gov.br/bvs/saudelegis/anvisa/2017/rdc0166\\_24\\_07\\_2017.pdf](https://bvsms.saude.gov.br/bvs/saudelegis/anvisa/2017/rdc0166_24_07_2017.pdf) (accessed 2025-02-03).
- (26) Marson, B.; Concentino, V.; Junkert, A.; Fachi, M.; Vilhena, R.; Pontarolo, R. Validation of analytical methods in a pharmaceutical quality system: An overview focused on HPLC methods. *Quim. Nova* **2020**, *43* (8), 1190-1203. <https://doi.org/10.21577/0100-4042.20170589>
- (27) Dewi, M.; Pratama, R.; Arifka, M.; Chaerunisaa, A. Quality by Design: Approach to Analytical Method Validation. *Sciences of Pharmacy* **2022**, *1* (1), 38–46. <https://doi.org/10.58920/sciphar01010033>
- (28) Zacharis, C. K.; Vastardi, E. Application of analytical quality by design principles for the determination of alkyl *p*-toluenesulfonates impurities in Aprepitant by HPLC. Validation using total-error concept. *J. Pharm. Biomed. Anal.* **2018**, *150*, 152–161. <https://doi.org/10.1016/j.jpba.2017.12.009>
- (29) Separovic, L.; Lourenço, F. R. Measurement Uncertainty Evaluation of an Analytical Procedure for Determination of Terbinafine Hydrochloride in Creams by HPLC and Optimization Strategies Using Analytical Quality by Design. *Microchem. J.* **2022**, *178*. <https://doi.org/10.1016/j.microc.2022.107386>
- (30) Kannaiah, K. P.; Sugumaran, A. Environmental Benign AQbD Based Estimation of Ketoconazole and Beclomethasone by RP-HPLC and Multi-Analytical UV Spectrophotometric Method. *Microchem. J.* **2022**, *172*. <https://doi.org/10.1016/j.microc.2021.106968>
- (31) Tai, Y.; Ren, D.; Zhao, W.; Qu, H.; Xiong, H.; Gong, X. Analytical Quality by Design Oriented Development of the UPLC Method for Analysing Multiple Pharmaceutical Process Intermediates: A Case Study of Compound Danshen Dripping Pills. *Microchem. J.* **2023**, *187*. <https://doi.org/10.1016/j.microc.2023.108438>
- (32) Sahu, P. K.; Ramiseti, N. R.; Cecchi, T.; Swain, S.; Patro, C. S.; Panda, J. An Overview of Experimental Designs in HPLC Method Development and Validation. *J. Pharm. Biomed. Anal.* **2018**, *147*, 590–611. <https://doi.org/10.1016/j.jpba.2017.05.006>
- (33) Tome, T.; Žigart, N.; Časar, Z.; Obreza, A. Development and Optimization of Liquid Chromatography Analytical Methods by Using AQbD Principles: Overview and Recent Advances. *Org. Process Res. Dev.* **2019**, *23* (9), 1784–1802. <https://doi.org/10.1021/acs.oprd.9b00238>
- (34) Breitzkreitz, M. Analytical Quality by Design. *Braz. J. Anal. Chem.* **2021**, *8* (32), 1–5. <https://doi.org/10.30744/brjac.2179-3425.editorial.mcbreitzkreitz.N32>
- (35) Saini, S.; Sharma, T.; Patel, A.; Kaur, R.; Tripathi, S. K.; Katore, O. P.; Singh, B. QbD-Steered Development and Validation of an RP-HPLC Method for Quantification of Ferulic Acid: Rational Application of Chemometric Tools. *J. Chrom. B* **2020**, *1155*. <https://doi.org/10.1016/j.jchromb.2020.122300>
- (36) Salwa, K. L. Quality-by-Design Driven Analytical Method (AQbD) Development and Validation of HPLC–UV Technique to Quantify Rivastigmine Hydrogen Tartrate in Lipidic Nanocarriers: Forced Degradation, and Assessment of Drug Content and in Vitro Release Studies. *Microchem. J.* **2023**, *193*. <https://doi.org/10.1016/j.microc.2023.108944>

## SUPPLEMENTARY MATERIAL

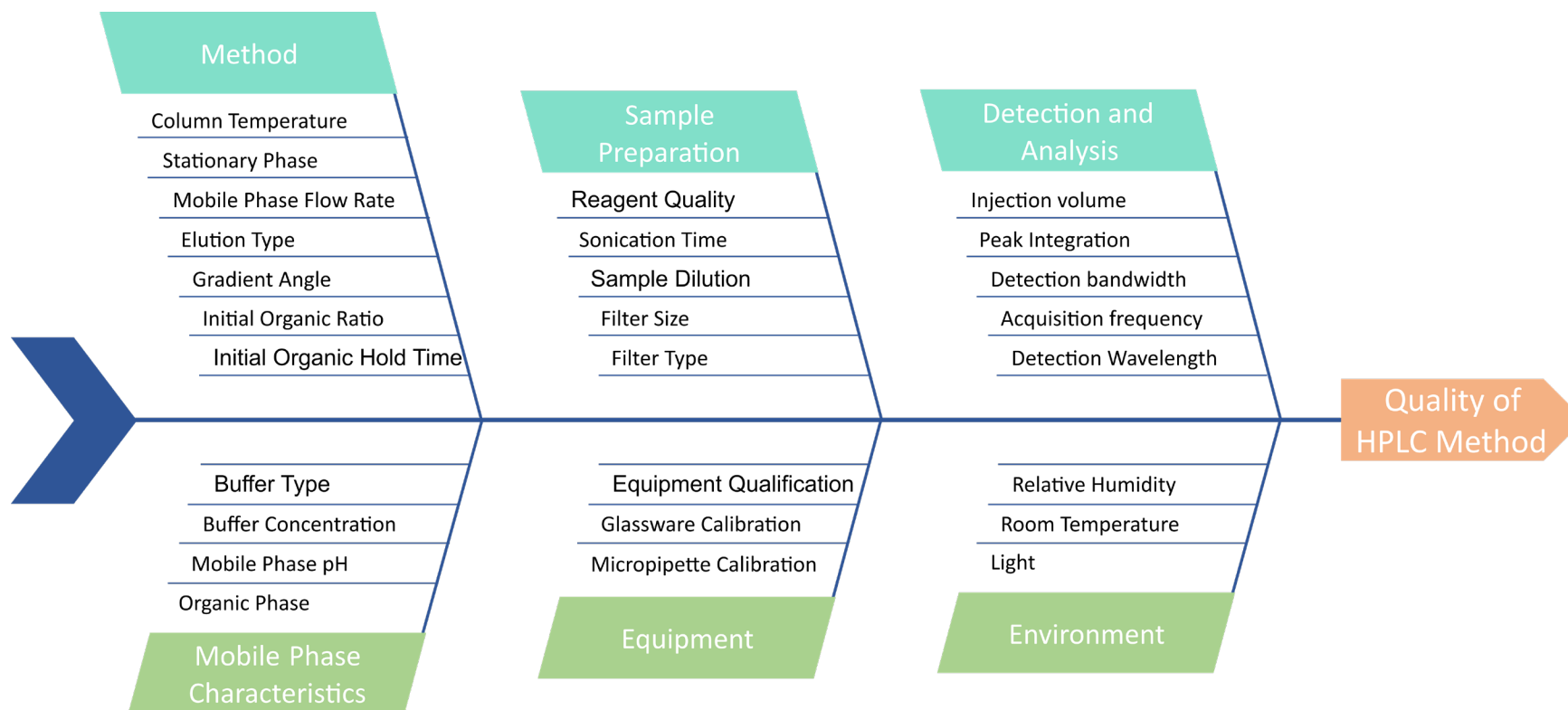


**Figure S1.** Ishikawa Diagram of Potential Critical Method Parameters.

**Table SI.** Risk Assessment Evaluation. Risk priority number thresholds: >225 (high risk), 224–175 (unacceptable), 174–125 (need evaluation), 124–50 (acceptable), and <50 (negligible).

| Category                     | CMP                       | Occurrence | Severity | Detection | Risk priority number | Corrective action or exclusion justification                          |
|------------------------------|---------------------------|------------|----------|-----------|----------------------|---|
| Method                       | Elution Type              | 1          | 10       | 1         | 10                   | Evaluated and defined in preliminary tests                            |
|                              | Initial Organic Ratio     | 1          | 7        | 5         | 35                   | Evaluated and defined after the screening tests                       |
|                              | Initial Organic Hold Time | 2          | 7        | 4         | 56                   | Evaluated and defined after the screening tests                       |
|                              | Gradient Slope            | 3          | 10       | 6         | 180                  | Continuous parameter to be evaluated and modeled                      |
|                              | Stationary Phase          | 2          | 10       | 7         | 140                  | Categorical parameter to be tested and fixed                          |
|                              | Column Temperature        | 5          | 7        | 7         | 245                  | Continuous parameter to be evaluated and modeled                      |
|                              | Mobile Phase Flow Rate    | 6          | 8        | 8         | 384                  | Continuous parameter to be evaluated and modeled                      |
| Sample Preparation           | Filter Size               | 1          | 3        | 1         | 3                    | Defined according to sample volume                                    |
|                              | Filter Type               | 1          | 3        | 1         | 3                    | Defined according to sample type                                      |
|                              | Sonication time           | 1          | 5        | 5         | 25                   | Previously assessed and fixed in the sample preparation protocol      |
|                              | Reagent Quality           | 2          | 5        | 8         | 80                   | Supplier qualification  |
|                              | Sample Dilution           | 3          | 7        | 5         | 105                  | Previously assessed and fixed in the sample preparation protocol      |
| Detection and Analysis       | Peak Integration          | 2          | 3        | 3         | 18                   | Defined and fixed at the beginning of the acquisitions                |
|                              | Acquisition Frequency     | 3          | 4        | 4         | 48                   | Low impact on peak separation and quantification with good resolution |
|                              | Detection bandwidth       | 3          | 5        | 4         | 60                   | Defined and fixed at the beginning of the acquisitions                |
|                              | Detection Wavelength      | 3          | 7        | 6         | 126                  | Evaluated and defined in preliminary tests                            |
|                              | Injection Volume          | 6          | 7        | 7         | 294                  | Evaluated and defined in preliminary tests                            |
| Mobile Phase Characteristics | Buffer Concentration      | 5          | 3        | 5         | 75                   | Low impact on separation and quantification                           |
|                              | Organic Phase             | 3          | 9        | 6         | 162                  | Categorical parameter to be tested and fixed                          |
|                              | Buffer Type               | 3          | 9        | 6         | 162                  | Categorical parameter to be tested and fixed                          |
|                              | Mobile Phase pH           | 7          | 9        | 8         | 504                  | Continuous parameter to be evaluated and modeled                      |
| Equipment                    | Glassware Calibration     | 5          | 8        | 5         | 200                  | Check and calibrate glassware   |
|                              | Equipment Qualification   | 4          | 8        | 7         | 224                  | Check and calibrate equipment qualification                           |
|                              | Micropipette Calibration  | 4          | 8        | 7         | 224                  | Check and calibrate micropipette calibration                          |
| Environment                  | Room Temperature          | 3          | 3        | 4         | 36                   | Controlled room temperature   |
|                              | Relative Humidity         | 3          | 4        | 4         | 48                   | Parameter controlled in sample storage                                |
|                              | Light                     | 5          | 4        | 4         | 80                   | Parameter controlled in sample storage                                |

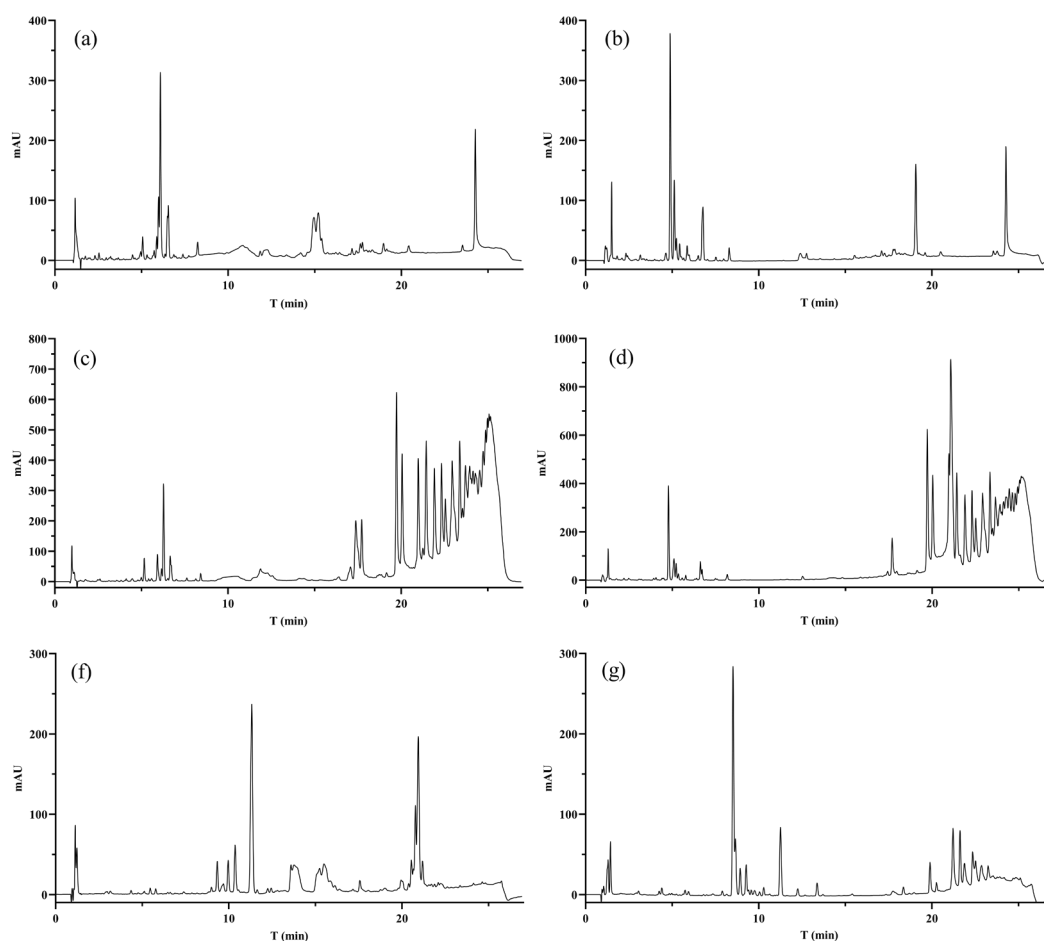


**Figure S2.** Screening test of categorical variables.

A - C8, ACN and acetate buffer; B - C8, ACN and formate buffer; C - C18, ACN and acetate buffer; D - C18, ACN and formate buffer; E - C18, MeOH and acetate buffer; F - C18, MeOH and formate buffer. The chromatographic analysis was performed using a Zorbax XBD C18 or XBridge BEH C8 column (150 × 4.6 mm, 3.5 μm). The mobile phase consisted of an ammonium acetate or ammonium formate buffer in combination with ACN or MeOH. A scouting gradient program was employed, with the following elution profile: 10%B at 0.0 min; 10-90%B from 0.0 to 24 min, and 90-10%B from 24 to 27 min. The flow rate was maintained at 1.5 mL/min throughout the analysis. The analysis was conducted at 25 °C, with a 40 μL injection volume, and detection at 254 nm.



**Table SII.** Results obtained from the Box-Behnken design. OCLA= Oclacitinib R= resolution factor, APR= Adjacent peak resolution factor, T= Tailing factor, and K'= Retention coefficient

| n  | A: Gradient slope      | B: Flow rate         | C: Buffer pH | D: Temperature | OCLA's R | OCLA's APR | OCLA's T | Last Peak K' |
|----|------------------------|----------------------|--------------|----------------|----------|------------|----------|--------------|
|    | [%B] min <sup>-1</sup> | mL min <sup>-1</sup> |              | °C             |          |            |          |              |
| 1  | 0.8                    | 1                    | 3.1          | 17.5           | 3.895    | 3.503      | 1.323    | 19.87        |
| 2  | 1.2                    | 1                    | 3.1          | 17.5           | 3.069    | 3.307      | 1.3      | 16.44        |
| 3  | 0.8                    | 1.4                  | 3.1          | 17.5           | 4.215    | 3.241      | 1.325    | 25.37        |
| 4  | 1.2                    | 1.4                  | 3.1          | 17.5           | 3.451    | 3.106      | 1.271    | 20.87        |
| 5  | 1                      | 1.2                  | 3            | 15             | 5.273    | 2.929      | 1.347    | 20.43        |
| 6  | 1                      | 1.2                  | 3.2          | 15             | 3.275    | 3.332      | 1.226    | 20.76        |
| 7  | 1                      | 1.2                  | 3            | 20             | 4.499    | 3.053      | 1.33     | 19.70        |
| 8  | 1                      | 1.2                  | 3.2          | 20             | 2.487    | 3.510      | 1.278    | 19.96        |
| 9  | 0.8                    | 1.2                  | 3.1          | 15             | 4.448    | 3.263      | 1.29     | 22.62        |
| 10 | 1.2                    | 1.2                  | 3.1          | 15             | 3.595    | 3.124      | 1.291    | 18.97        |
| 11 | 0.8                    | 1.2                  | 3.1          | 20             | 3.647    | 3.385      | 1.351    | 22.18        |
| 12 | 1.2                    | 1.2                  | 3.1          | 20             | 2.986    | 3.264      | 1.279    | 18.34        |
| 13 | 1                      | 1                    | 3            | 17.5           | 4.758    | 3.130      | 1.35     | 17.51        |
| 14 | 1                      | 1.4                  | 3            | 17.5           | 4.778    | 2.884      | 1.331    | 22.11        |
| 15 | 1                      | 1                    | 3.2          | 17.5           | 2.672    | 3.530      | 1.264    | 17.80        |
| 16 | 1                      | 1.4                  | 3.2          | 17.5           | 3.119    | 3.289      | 1.243    | 22.84        |
| 17 | 0.8                    | 1.2                  | 3            | 17.5           | 5.180    | 3.075      | 1.343    | 20.90        |
| 18 | 1.2                    | 1.2                  | 3            | 17.5           | 4.482    | 2.981      | 1.338    | 18.21        |
| 19 | 0.8                    | 1.2                  | 3.2          | 17.5           | 3.210    | 3.553      | 1.298    | 22.73        |
| 20 | 1.2                    | 1.2                  | 3.2          | 17.5           | 2.651    | 3.368      | 1.207    | 18.80        |
| 21 | 1                      | 1                    | 3.1          | 15             | 3.676    | 3.302      | 1.266    | 18.04        |
| 22 | 1                      | 1.4                  | 3.1          | 15             | 4.017    | 3.060      | 1.282    | 22.62        |
| 23 | 1                      | 1                    | 3.1          | 20             | 3.098    | 3.480      | 1.285    | 17.36        |
| 24 | 1                      | 1.4                  | 3.1          | 20             | 3.299    | 3.278      | 1.285    | 22.21        |
| 25 | 1                      | 1.2                  | 3.1          | 17.5           | 3.572    | 3.264      | 1.288    | 20.04        |
| 26 | 1                      | 1.2                  | 3.1          | 17.5           | 3.592    | 3.248      | 1.32     | 20.10        |
| 27 | 1                      | 1.2                  | 3.1          | 17.5           | 3.548    | 3.252      | 1.271    | 20.49        |
| 28 | 1                      | 1.2                  | 3.1          | 17.5           | 3.534    | 3.314      | 1.318    | 19.79        |

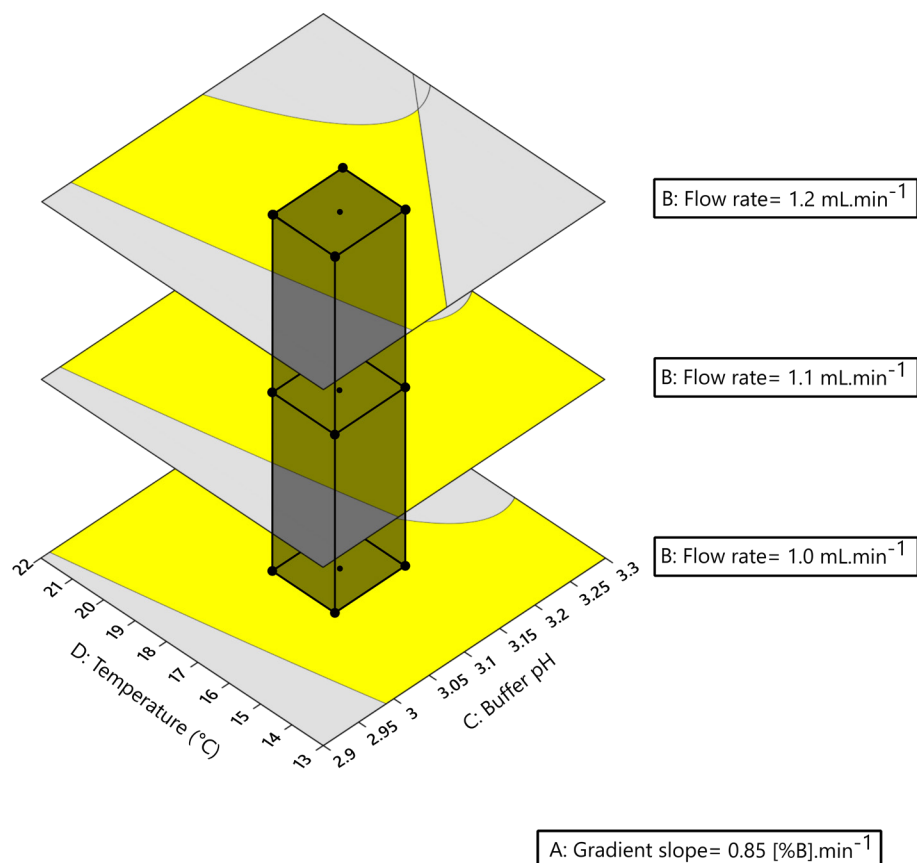


**Figure S3.** Combination of overlay plots at three flow rate levels. The Method Operable Design Range (MODR) are represented by the yellow area, the translucent parallelepiped delineates the Proven Acceptable Ranges (PARs) and the dots indicates each point that were tested.

**Table SIII.** Results from Proven Acceptable Ranges for model validation. OCLA= Oclacitinib R= resolution factor, APR= Adjacent peak resolution factor, T= Tailing factor, and K'= Retention coefficient

|            | A: Gradient slope      | B: Flow rate         | C: Buffer pH | D: Temperature | OCLAs R    |          |             | OCLA's APR |          |             | OCLA's T   |          |             | Last Peak K' |          |             |
|------------|------------------------|----------------------|--------------|----------------|------------|----------|-------------|------------|----------|-------------|------------|----------|-------------|--------------|----------|-------------|
| PAR Points | [%B] min <sup>-1</sup> | mL min <sup>-1</sup> |              | °C             | 95% TI Low | Measured | 95% TI High | 95% TI Low | Measured | 95% TI High | 95% TI Low | Measured | 95% TI High | 95% TI Low   | Measured | 95% TI High |
| PAR 1      | 0.85                   | 1                    | 3.05         | 16.0           | 4.166      | 4.331    | 4.895       | 3.161      | 3.270    | 3.394       | 1.254      | 1.371    | 1.380       | 17.32        | 18.20    | 20.77       |
| PAR 2      | 0.85                   | 1                    | 3.05         | 18.0           | 3.899      | 4.231    | 4.620       | 3.227      | 3.353    | 3.457       | 1.268      | 1.405    | 1.388       | 17.32        | 17.98    | 20.77       |
| PAR 3      | 0.85                   | 1                    | 3.15         | 16.0           | 3.088      | 3.556    | 3.817       | 3.372      | 3.522    | 3.605       | 1.216      | 1.351    | 1.342       | 17.65        | 19.15    | 21.11       |
| PAR 4      | 0.85                   | 1                    | 3.15         | 18.0           | 2.821      | 3.325    | 3.542       | 3.438      | 3.562    | 3.668       | 1.244      | 1.348    | 1.364       | 17.65        | 19.18    | 21.11       |
| PAR 5      | 0.85                   | 1                    | 3.10         | 17.0           | 3.428      | 4.032    | 4.131       | 3.314      | 3.422    | 3.544       | 1.249      | 1.317    | 1.365       | 17.50        | 18.73    | 20.92       |
| PAR 6      | 0.85                   | 1.1                  | 3.05         | 16.0           | 4.231      | 4.436    | 4.927       | 3.107      | 3.191    | 3.333       | 1.254      | 1.317    | 1.380       | 18.58        | 20.02    | 21.92       |
| PAR 7      | 0.85                   | 1.1                  | 3.05         | 18.0           | 3.965      | 4.159    | 4.651       | 3.172      | 3.262    | 3.395       | 1.268      | 1.359    | 1.388       | 18.58        | 19.39    | 21.92       |
| PAR 8      | 0.85                   | 1.1                  | 3.15         | 16.0           | 3.207      | 3.671    | 3.903       | 3.317      | 3.470    | 3.544       | 1.216      | 1.315    | 1.342       | 18.92        | 20.70    | 22.26       |
| PAR 9      | 0.85                   | 1.1                  | 3.15         | 18.0           | 2.940      | 3.375    | 3.627       | 3.383      | 3.503    | 3.606       | 1.244      | 1.333    | 1.364       | 18.92        | 20.37    | 22.26       |
| PAR 10     | 0.85                   | 1.2                  | 3.05         | 16.0           | 4.287      | 4.628    | 4.970       | 3.050      | 3.194    | 3.274       | 1.254      | 1.383    | 1.380       | 19.81        | 20.81    | 23.11       |
| PAR 11     | 0.85                   | 1.2                  | 3.05         | 18.0           | 4.021      | 4.227    | 4.693       | 3.116      | 3.203    | 3.336       | 1.268      | 1.380    | 1.388       | 19.81        | 20.24    | 23.11       |
| PAR 12     | 0.85                   | 1.2                  | 3.15         | 16.0           | 3.315      | 3.700    | 3.998       | 3.261      | 3.330    | 3.484       | 1.216      | 1.335    | 1.342       | 20.15        | 21.94    | 23.45       |
| PAR 13     | 0.85                   | 1.2                  | 3.15         | 18.0           | 3.049      | 3.450    | 3.722       | 3.326      | 3.424    | 3.547       | 1.244      | 1.338    | 1.364       | 20.15        | 20.40    | 23.45       |
| PAR 14     | 0.85                   | 1.2                  | 3.10         | 17.0           | 3.594      | 4.053    | 4.266       | 3.203      | 3.205    | 3.423       | 1.249      | 1.262    | 1.365       | 20.01        | 21.08    | 23.25       |
| NOC        | 0.85                   | 1.1                  | 3.10         | 17.0           | 3.514      | 4.069    | 4.195       | 3.259      | 3.333    | 3.482       | 1.249      | 1.294    | 1.365       | 18.77        | 20.23    | 22.07       |
| NOC        | 0.85                   | 1.1                  | 3.10         | 17.0           | 3.514      | 4.072    | 4.195       | 3.259      | 3.333    | 3.482       | 1.249      | 1.315    | 1.365       | 18.77        | 20.23    | 22.07       |
| NOC        | 0.85                   | 1.1                  | 3.10         | 17.0           | 3.514      | 4.081    | 4.195       | 3.259      | 3.333    | 3.482       | 1.249      | 1.320    | 1.365       | 18.77        | 20.23    | 22.07       |

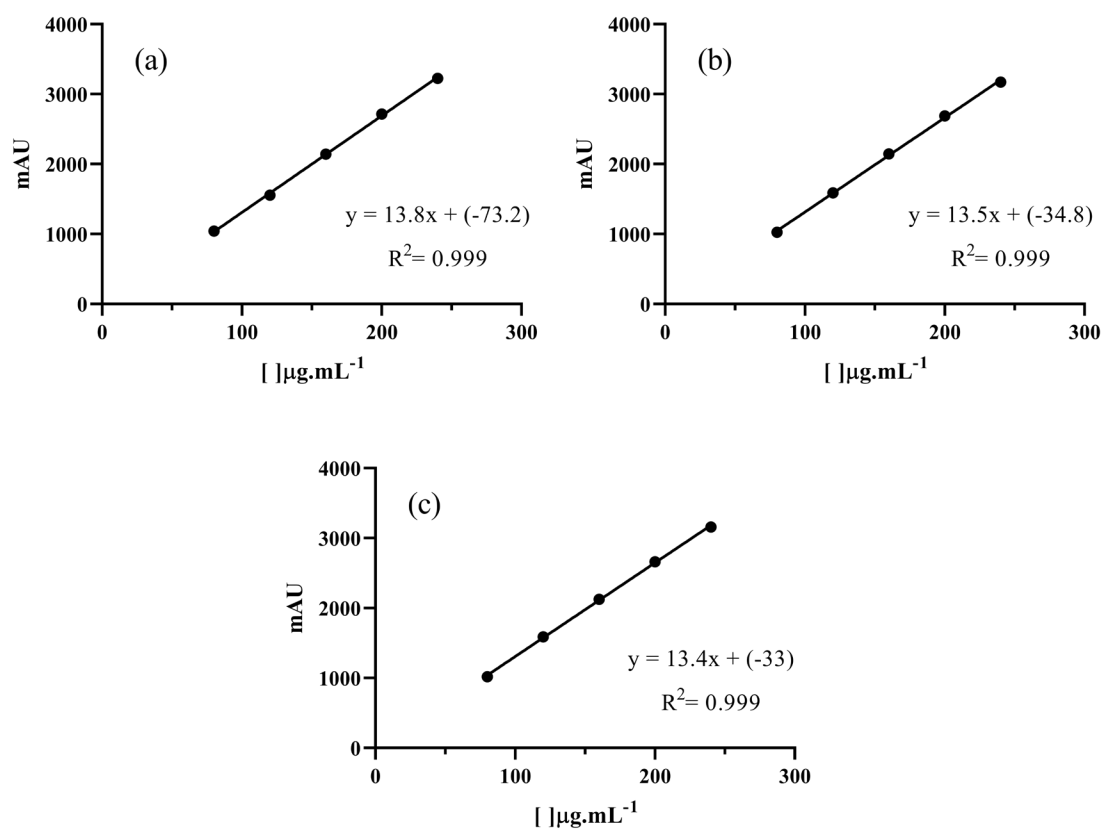


Figure S4. Linearity calibration curves A, B and C.

Table SIV. Repeatability results. SD = standard deviation, RSD = relative standard deviation

| Concentration<br>( $\mu\text{g mL}^{-1}$ ) | Area   | Mean   | SD    | RSD   |
|--|--------|--------|-------|-------|
| 80   | 1038.8 | 1035.9 | 11.67 | 1.13% |
|  | 1023.1 |        |       |       |
|  | 1045.9 |        |       |       |
| 160  | 2116.4 | 2132.1 | 37.21 | 1.75% |
|  | 2105.4 |        |       |       |
|  | 2174.6 |        |       |       |
| 240  | 3168.4 | 3174.6 | 32.35 | 1.02% |
|  | 3145.8 |        |       |       |
|  | 3209.6 |        |       |       |

**Table SV.** Intermediate precision results. Note: SD = standard deviation, RSD = relative standard deviation.

| Concentration<br>( $\mu\text{g mL}^{-1}$ ) | Analyst 1 | Analyst 2 | Mean   | SD    | RSD   | Test <i>t</i><br>(p-value) | Test F<br>(p-value) |
|--|-----------|-----------|--------|-------|-------|----------------------------|---------------------|
| 80   | 1072.1    | 1025.0    | 1041.7 | 18.20 | 1.75% | 0.090                      | 0.656               |
|  | 1046.5    | 1021.1    |        |       |       |                            |                     |
|  | 1043.4    | 1041.8    |        |       |       |                            |                     |
| 160  | 2176.9    | 2133.7    | 2126.1 | 33.91 | 1.60% | 0.308                      | 0.578               |
|  | 2099.7    | 2084.2    |        |       |       |                            |                     |
|  | 2148.4    | 2113.5    |        |       |       |                            |                     |
| 240  | 3217.6    | 3211.8    | 3178.7 | 39.38 | 1.24% | 0.505                      | 0.985               |
|  | 3143.0    | 3132.1    |        |       |       |                            |                     |
|  | 3212.4    | 3155.0    |        |       |       |                            |                     |

**Table SVI.** Accuracy results. SD = standard deviation, RSD = relative standard deviation, CI = confidence interval.

| Level  | ( $\mu\text{g mL}^{-1}$ ) | Theoretical area |                   |       | Observed area |                   |       | Recovery $\pm$ CI<br>(95%) |
|--------|---------------------------|------------------|-------------------|-------|---------------|-------------------|-------|----------------------------|
|        |                           | Area             | Mean $\pm$ SD     | RSD   | Area          | Mean $\pm$ SD     | RSD   |                            |
| Low    | 80                        | 1058.7           | 1060.2 $\pm$ 16.3 | 1.54% | 1035.3        | 1039.5 $\pm$ 14.4 | 1.67% | 98.05% $\pm$ 0.14%         |
|        |                           | 1077.2           |                   |       | 1058.6        |                   |       |                            |
|        |                           | 1044.6           |                   |       | 1024.6        |                   |       |                            |
| Medium | 160                       | 2164.5           | 2167.4 $\pm$ 32.6 | 1.51% | 2172.9        | 2164.0 $\pm$ 27.3 | 1.26% | 99.85% $\pm$ 0.32%         |
|        |                           | 2201.4           |                   |       | 2185.9        |                   |       |                            |
|        |                           | 2136.3           |                   |       | 2133.4        |                   |       |                            |
| High   | 240                       | 3270.2           | 3274.6 $\pm$ 49.0 | 1.50% | 3216.5        | 3244.2 $\pm$ 37.4 | 1.15% | 99.07% $\pm$ 0.50%         |
|        |                           | 3325.6           |                   |       | 3286.8        |                   |       |                            |
|        |                           | 3227.9           |                   |       | 3229.2        |                   |       |                            |